Milestone Transactions on
MEDICAL TECHNOMETRICS
Vol. 03, Issue. 01, 2025

RESEARCH ARTICLE OPEN ACCESS

Automated Tuberculosis Detection from Chest X-Rays Using a ResNet50 Architecture

Sreelakshmi Induri[1] . M Reddi Durgasree[2] . Beeda Sukumar[3] . G Ramasubba Reddy[4] . Y Subba Reddy[4] . J Jagadeswara Reddy[4]

[1]Department of Computer Science, St. Francis College for Women, Begumpet, Hyderabad, India
[2]Department of CSE (AI&ML), Guru Nanak Institutions Technical Campus, Hyderabad, India
[3]Department of ECE, Narayana Engineering College, Nellore, India
[4]Department of Computer Science Engineering, Sai Rajeswari Institute of Technology, Proddatur, Andhra Pradesh, India.

DOI: **10.5281/zenodo.14903623**
Received: 23 January 2025 / Revised: 12 February 2025 / Accepted: 19 February 2025

Abstract – TB (tuberculosis) is still a major worldwide health concern, and in order to control its spread and enhance patient outcomes, precise and prompt diagnostic methods are required. This study introduces a deep-learning methodology employing a ResNet50 architecture for the reliable and precise classification of TB in CXR images. The model utilizes a robust CNN (Convolutional Neural Network) to extract essential features, enhanced by image pre-processing techniques to optimize image quality and overall performance. The ResNet50 classifier shows great performance metrics, achieving an accuracy of 99.82%, a 99.82% accuracy rate and an AUC of 99.87%. These results highlight the potential of ResNet50 as a valuable TB detection tool for healthcare professionals, particularly in resource-constrained environments, enabling faster diagnosis and treatment.

Index Terms – TB Diagnosis, Deep Learning, Chest X-Rays, Interpretability, LIME, ResNet50.

I. INTRODUCTION

As one of the most prevalent infectious disease-related causes of death is TB. Although drug treatments are available, particularly benefiting rural and resource-limited areas, TB is sometimes misdiagnosed and consequently left untreated [1]. The lungs, which are essential organs of the respiratory system, facilitate gas exchange during breathing. Numerous diseases can compromise the respiratory

MILESTONE RESEARCH.IN OPEN ACCESS
Electronic ISSN: **2584-072X**

Milestone Transactions on
MEDICAL TECHNOMETRICS
Vol. 03, Issue. 01, 2025

system and interfere with its function [2], with TB being a significant concern [3]. Additionally, TB might impact other bodily components, including the brain and spine [4]. The WHO (World Health Organization) considers TB a life-threatening illness, and their reports indicate a progressive rise in the yearly death toll from TB [5].

Traditional clinical assessments, such as physical examinations and patient histories, often lack the precision required for accurate TB identification. Subtle or uncommon symptoms can be easily overlooked, leading to delayed or missed diagnoses. In contrast, chest X-ray (CXR) imaging offers a more reliable and dependable method for detecting lung abnormalities indicative of TB. Medical professionals can identify a range of respiratory system disorders through CXR analysis [6]. TB, a recurring infectious disease, caused approximately 1.5 million deaths globally in 2020, emphasizing the critical need for early and precise detection to curb its spread and reduce mortality. CXR remains one of the most frequently used diagnostic tools for tuberculosis detection [7].

Recent research has increasingly focused on utilizing deep Convolutional Neural Network (CNN) [10] models to identify lung abnormalities, including lung cancer, pneumonia, and TB, from CXR images. Similarly, conventional machine learning (ML) techniques have been employed in various studies to differentiate between TB, healthy lungs, and other non-TB lung diseases using CXR images. Despite the diagnostic benefits of CNN models, they may sometimes miss subtle or atypical TB patterns. Furthermore, the use of diverse, high-quality datasets and hierarchical feature extraction can lead to large trends that obscure finer diagnostic information. To address these limitations, researchers have developed deep CNN models using network pruning strategies to enhance TB detection.

Traditional machine learning (ML) models also have their limitations [12]. They require time-consuming and domain-specific feature engineering. Unlike deep learning models, ML algorithms may struggle to interpret complex, non-linear relationships within the data. While deep learning algorithms excel in many areas, they can underperform with high-dimensional data, such as images. Both approaches often struggle to balance accuracy and computational effectiveness, especially in situations with limited resources or in real time. The use of a ResNet50 architecture for automatic TB detection from CXR pictures is investigated in this work [8] [9]. The motivation is to raise the efficiency and accuracy of TB detection using advanced DL techniques while ensuring that the model remains computationally efficient for real-world scenarios. The ResNet50 classifier demonstrates exceptional performance measures with recall, precision, accuracy, and f1-score that is highly aligned with the contribution to this study and is of 99.82%, along with an AUC of 99.87%.

II. LITERATURE SURVEY

Tuberculosis remains a huge global public health concern., resulting in substantial morbidity and mortality. The WHO identifies tuberculosis as one of the foremost infectious diseases, highlighting how crucial early discovery is to successful treatment and management. Traditional diagnostic methods, including sputum smear microscopy, chest X-ray (CXR) analysis, and molecular tests such as GeneXpert and PCR, have been widely used. However, these approaches are limited by factors such as insufficient sensitivity, the requirement for specialized human expertise, high implementation costs, and limited availability in resource-constrained settings. The use of AI (artificial intelligence), especially deep

Milestone Transactions on
MEDICAL TECHNOMETRICS
Vol. 03, Issue. 01, 2025

learning technologies, has increased recently, for the automated detection of TB has shown considerable promise, leveraging sophisticated image analysis techniques on CXR images. Several research teams have classified CXR images into TB and non-TB cases using conventional machine-learning techniques [13]. By fine-tuning the parameters of deep-layer CNN, a variety of DL methods have been applied more recently to identify tuberculosis [11]. One study found that a computer-aided technique that employed CNNs and intelligent pattern recognition was able to diagnose tuberculosis from CXR images with an accuracy of 88.76% [14]. Using a transfer learning technique, another study detected tuberculosis with 94.89% accuracy [15]. Furthermore, a CNN ensemble-based approach for the automatic categorization of tuberculosis from X-ray images was introduced, showing an 86% accuracy rate. [16].

A pre-trained CNN model that is generalized for TB detection has also been proposed [17] with and without image augmentation, this model achieved accuracies of 81.25% and 80%, respectively. Other researchers utilized pre-trained CNNs, including ChexNet and DenseNet201, for detection accuracies of 96.47% and 98.6% [10], respectively, highlighting the general performance of segmentation in enhancing diagnostic performance. Furthermore, visualization techniques like Score-CAM have been used to ensure that the model's decision-making is primarily based on lung regions, thus reinforcing the approach. One study evaluated five AI algorithms for TB detection from chest X-rays, with accuracies reaching as high as 95%. There is a growing shift from traditional clinical methods of TB detection toward AI-based solutions, which have demonstrated significant advancements in diagnostic capabilities. While CNN-based models have shown remarkable accuracy in automating TB diagnosis, challenges related to dataset diversity, model interpretability, and deployment feasibility remain. To address these limitations, the present study explores the application of a ResNet50 architecture, aiming to revolutionize TB detection through a fast and accurate AI-driven diagnostic tool, building upon the foundation laid by previous research.

III. PROPOSED METHODOLOGY

The methodologies used in this investigation are described in depth in this section. It contains explanations of the ResNet50 model's design, preprocessing methods, and dataset used. A visual representation of the entire workflow is given in Figure 1.

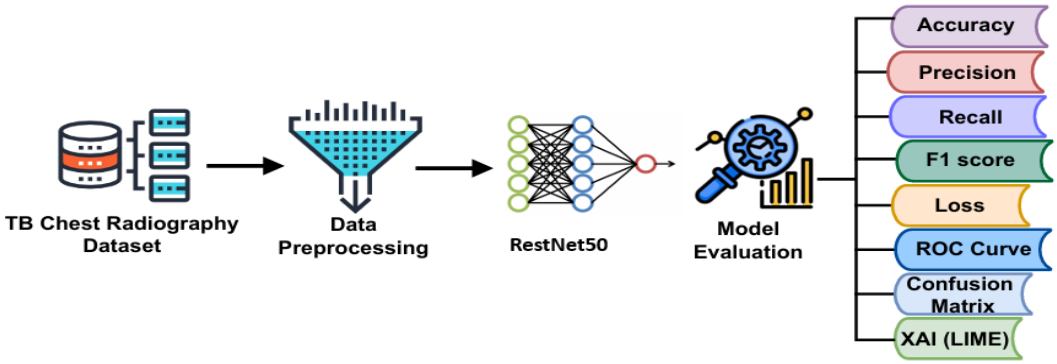

Fig. 1: Overview of the proposed workflow, from dataset acquisition to classification

Milestone Transactions on
MEDICAL TECHNOMETRICS
Vol. 03, Issue. 01, 2025

A. Dataset Description

This work makes use of the TB Chest Radiography dataset from Kaggle, a publicly accessible resource for TB categorization research. Images in the dataset are divided into two main categories: normal cases and TB-positive patients. 700 TB-positive chest X-ray photos are included in the publicly available dataset, along with 3500 normal chest X-ray images that served as a control group. Researchers can also obtain an additional 2800 TB-positive image sets through an agreement with the NIAID TB portal, further enhancing the dataset for more comprehensive analysis. To ensure a balanced representation of both classes, the data is oversampled to achieve a 3500:3500 ratio. The dataset is then separated into three sections: testing (10%), validation (10%), and training (80%). This partitioning ensures a robust model assessment and reliable performance evaluation[18].

B. Dataset Preprocessing:

1) *Image Conversion:* The initial step in preparing the data involves image conversion, where the raw dataset, consisting of PNG files, is transformed into a NumPy array. NumPy arrays, which are essentially matrices optimized for mathematical operations, facilitate efficient data translation and processing. Each image is initially stored in a specific file format and is now represented as a NumPy array with dimensions H × W × C (height, width, channels), where C represents the color channels (typically 3 for RGB images). This array format is fundamental for model input, enhancing processing and management.
2) *Image Resizing:* To address variations in image dimensions, images are resized to a consistent size of 128x128 pixels from their original 512x512 resolution. This scaling ensures uniform image ratios across all images, making them suitable for batch processing during model construction. Interpolation methods, such as bilinear interpolation, are employed to reduce the image size from 512×512 to 128×128 while preserving essential features and minimizing computational cost.
3) *Normalizing Pixel Values:* Pixel values are normalized to the range 1, further standardizing the data. This step is crucial for practical training as it enables the model to converge stably and more rapidly. Initially ranging from 0 to 255, the pixel values are scaled to the 1 range by dividing by 255, reducing sensitivity to pixel intensity variations and optimizing the overall learning process.
4) *Image Enhancement:* To increase the visual quality of the photos, a variety of image enhancement techniques are used. Contrast stretching enhances image contrast by expanding the range of pixel intensity values across the entire available range. The contrast stretching formula ensures that the original intensity values are mapped to a larger scale, enhancing the distinctiveness of features and supporting feature extraction. Additionally, histogram equalization aids in image contrast adjustment by uniformly spreading pixel intensities throughout the given range. Remapping the intensity values using the cumulative distribution function (or CDF) does this.By applying histogram equalization to smaller areas of the image, adaptive histogram equalization increases local contrast by emphasizing features that might be obscured by global changes. To prevent noise overamplification, Contrast Limited Adaptive Histogram Equalization (CLAHE) is often used in homogeneous areas.

Milestone Transactions on
MEDICAL TECHNOMETRICS
Vol. 03, Issue. 01, 2025

C. ResNet50 Architecture

Figure 2 provides a detailed illustration of the ResNet50 model's architecture, which consists of 9 layers.

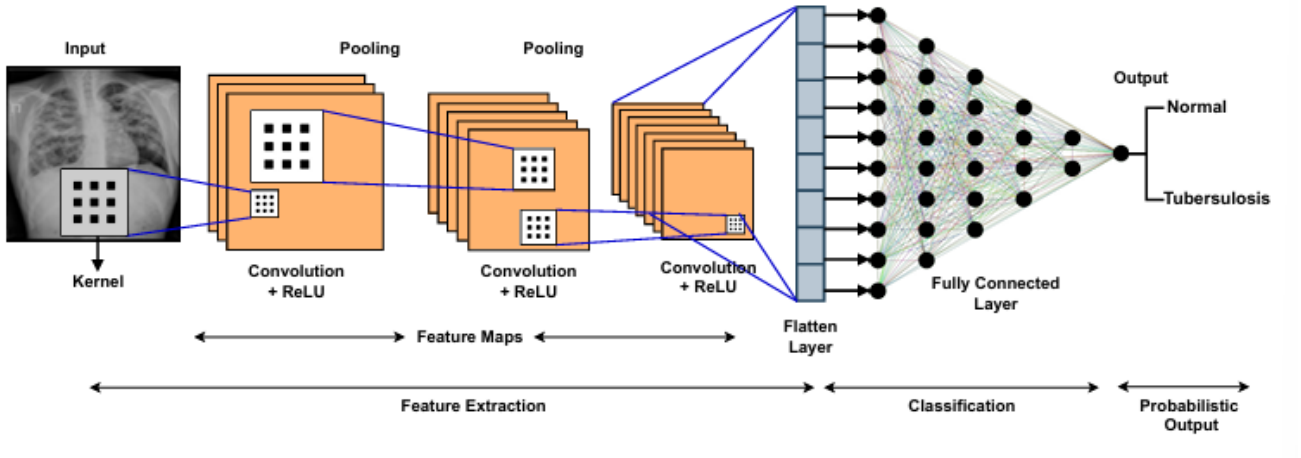

Fig. 2: Architecture of the Advanced TBNet Classifier model

1) *Input Layer:* The ResNet50 model accepts 224, 224, 3 shaped input pictures. The network is fed these pictures in order to extract features.
2) *Convolutional Layers and Residual Blocks:* Each residual block has ReLU activation functions, batch normalization layers, and convolutional layers. There are multiple stages in the ResNet50 architecture, and each one has a number of residual blocks. These phases gradually increase the number of feature channels while decreasing the feature maps' spatial dimensions. As a result, the network can record features at various complexities and scales.

$$O = \text{ReLU}(W * X + b)$$
$$\text{ReLU}(z) = \max(0, z)$$

where X is the input (an image or feature map), W is the filter weights, O is the output, b is the bias term, and $*$ indicates the convolution process.

3) *Pooling Layers:* By reducing the spatial dimensions of the feature maps, pooling layers lower computational cost and boost the network's resistance to spatial fluctuations in the input images. In ResNet50, max pooling is frequently utilized.

$$P = \text{Pooling}(O)$$

where P, the pooled result, reduces the feature maps' spatial dimensions

4) *Fully Connected Layer:* The feature maps are input into a fully connected layer after being flattened into a 1-dimensional vector by the convolutional and pooling layers. This layer associates the output classes (TB positive or negative) with the learned characteristics. The model's confidence in the positive class (TB positive) is then represented as a probability between 0 and 1, this is acquired by running a sigmoid activation function through the fully linked layer's output.
5) *Output Layer:* A single unit with a sigmoid activation function makes up the last layer of the ResNet50 model, producing a probability between 0 and 1. This probability reflects the model's confidence in the positive class (TB positive). The computation is as follows:

$$y = \sigma(W \times D + b)$$

Milestone Transactions on
MEDICAL TECHNOMETRICS
Vol. 03, Issue. 01, 2025

where:
The sigmoid activation function σ is,
y is the final prediction,
W is the output layer weights and b is biases, respectively.

6) *Regularization:* To avoid overfitting, regularization strategies like L1 and L2 regularization are employed. To stop the model from finding too intricate patterns that fit the noise in the training data, these methods include a penalty term in the loss function. The regularization terms are defined as:
L1 = λ1 |W|
L2 = λ2 W^2
where λ1 and λ2 are the regularization constants,
W is the weight matrix.

7) Optimizer: During training, the model's weights are modified using the Adam optimizer. Adam uses estimates of the gradients' first and second moments to modify the learning rates for each weight. The update rule for the optimizer parameters is as follows:
$\theta t+1 = \theta t - \eta * mt / (\sqrt{vt} + \varepsilon)$
where mt is gradient's moving averages and vt is squared gradient, θt is parameter at time step t, η is learning rate, and ε is a tiny constant to avoid division by zero.

8) Loss Function: To train the model, the binary cross-entropy loss function is employed. This loss function quantifies the discrepancy between the expected probability and the actual binary labels. Given N samples, the binary cross-entropy loss is calculated as:
$L = -1/N \Sigma [yi \log(\hat{y}i) + (1 - yi) \log(1 - \hat{y}i)]$
where:
The number of samples is N.
The true label is yi, and
The predicted probability is denoted by ηi.

IV. RESULTS AND DISCUSSIONS

The evaluation results of the ResNet50 model as a tuberculosis detection classifier are shown in this section.We give a thorough analysis of the model's performance, evaluating its accuracy in detecting TB cases using chest X-ray pictures. Key performance measures such the confusion matrix, F1 score, precision, accuracy, and recall are used to evaluate the model. Additionally, we examine loss and accuracy curves, The results can be fully understood thanks to the confusion matrix and ROC (Receiver Operating Characteristic) curves. The addition of LIME-based explainability provides more information about how the model makes decisions.

A. Comparative Analysis and Performance Metrics Evaluation

Table I shows the performance evaluation metrics of the ResNet50 model for identifying tuberculosis from chest X-ray pictures. With a score of 99.62%, the model exhibits excellent alignment with the actual labels and a high degree of prediction accuracy. This high accuracy shows that the ResNet50 model effectively reduces false positives and false negatives, ensuring reliable detection. The model has a low

Milestone Transactions on
MEDICAL TECHNOMETRICS
Vol. 03, Issue. 01, 2025

false-positive rate and accurately detects TB patients with a precision value of 99.63%. Reducing false positives is crucial in medical settings because they may cause unnecessary patient anxiety and additional testing.

TABLE I: Performance Metrics of the ResNet50 Regarding Tuberculosis Detection

Model	Accuracy(%)	Precision(%)	Recall(%)	F1-score(%)
ResNet50	99.62	99.63	99.62	99.62

Table I presents the performance evaluation scores for the ResNet50 model in identifying TB from chest X-ray images. The model achieves an accuracy of 99.62%, indicating a strong alignment with the actual labels in its predictions. This high accuracy indicates that the ResNet50 model can reduce false positives and false negatives, producing dependable detection results.The precision value is 99.63%, demonstrating the model's ability to correctly identify TB cases while minimizing false positive results. Reducing false positives is critical in clinical settings, as they can cause unnecessary patient anxiety and further diagnostic procedures. The model's effectiveness in identifying true TB cases is reflected in a recall value of 99.62%, crucial for accurate early detection and timely treatment. The F1-score, which balances precision and recall, is 99.62%, offering a comprehensive measure of performance. This metric is particularly important in scenarios with skewed datasets, as it indicates how well the model manages true/false positives and true/false negatives concurrently.

The ResNet50 model demonstrates strong performance, gaining an accuracy of 99.62%, which compares favorably to existing approaches such as UNet + Xception (99.29%) and EfficientNetB3 (99.10%). In comparison to the CNN, ANN, and RNN combination, which reported an F1-score of 88%, the ResNet50 model achieves an F1-score of 99.62%, indicating a notable performance improvement. The high accuracy of the ResNet50 model underscores its potential for effective tuberculosis classification in real-world automated diagnosis applications. The ResNet50 model demonstrates impressive strength as a promising solution for automated TB detection in medical settings. Given that precision and reliability are crucial in clinical deployment to healthcare facilities, the model demonstrates excellent performance capabilities. This successful outcome highlights how advancements in machine learning can enable better healthcare diagnostic systems, potentially delivering accessible TB screening worldwide.

B. Accuracy and Loss Curves during Training and Validation

The accuracy and loss curves, which show the ResNet50 model's development throughout 30 training and validation epochs, are shown in Figures 3 and 4, respectively. As the number of epochs rises, the training and validation accuracy curves show a steady improvement. Initially, the training accuracy curve (solid blue line) exhibits a rapid increase, indicating the model's quick adaptation to the training data patterns. The validation accuracy curve (dashed red line) follows a similar upward trend, with minor fluctuations, demonstrating the model's ability to generalize to new instances. The ResNet50 model achieves consistent accuracy gains, with the training and validation accuracy converging to approximately 99%. This indicates that the model effectively learned TB detection features and stabilized without significant overfitting.

Milestone Transactions on
MEDICAL TECHNOMETRICS
Vol. 03, Issue. 01, 2025

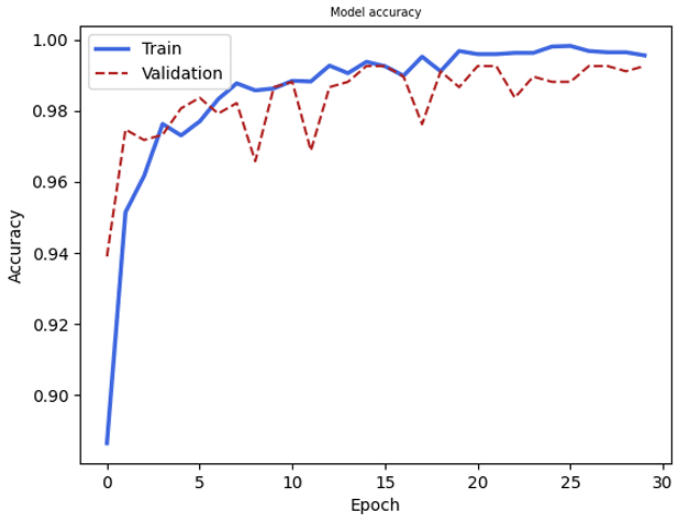

Fig. 3: Training and validation accuracy for the proposed ResNet50 over epochs

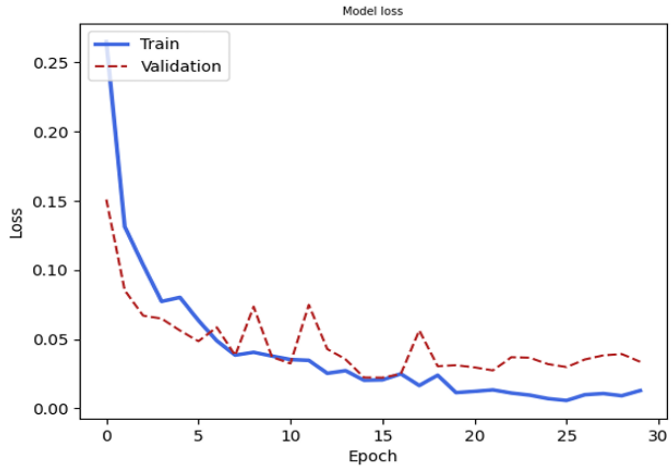

Fig. 4: Training and validation loss for the proposed ResNet50 over epochs

The loss curve in Figure 4 illustrates how the ResNet50 model reduces error during training and validation. The solid blue line, representing the training loss, starts at a high value and decreases as the model optimizes its parameters with each training epoch, indicating improved performance. Similarly, the validation loss (dashed red line) also decreases, with slight oscillations, reflecting variations in the model's ability to generalize across different epochs. As the training progresses, the training and validation loss values converge to low levels and stabilize, indicating that the ResNet50 model has reached convergence.

C. ROC Curve for the ResNet50 Model

By employing the ROC curve to illustrate the trade-off between sensitivity (true positive rate) and 1-specificity (false positive rate), Figure 5 offers a thorough assessment of the ResNet50 model's diagnostic performance. The model's dramatic climb along the y-axis indicates its high sensitivity, which approaches the top-left corner of the y-axis for different threshold values. This illustrates the classifier's ability to reduce false negatives while differentiating between TB-positive and TB-negative cases. Additionally, the ROC curve is clearly distinct from the diagonal baseline, which represents random

Milestone Transactions on
MEDICAL TECHNOMETRICS
Vol. 03, Issue. 01, 2025

guessing, demonstrating the model's effectiveness in distinguishing between classes. The consistent upward trend of the ROC curve shows the stability of the classifier's performance over time. For clinical applications, maintaining a balance between sensitivity and specificity is crucial to minimize both missed diagnoses and false alarms. Therefore, the ROC curve confirms the reliability and robustness of the ResNet50 model for TB detection.

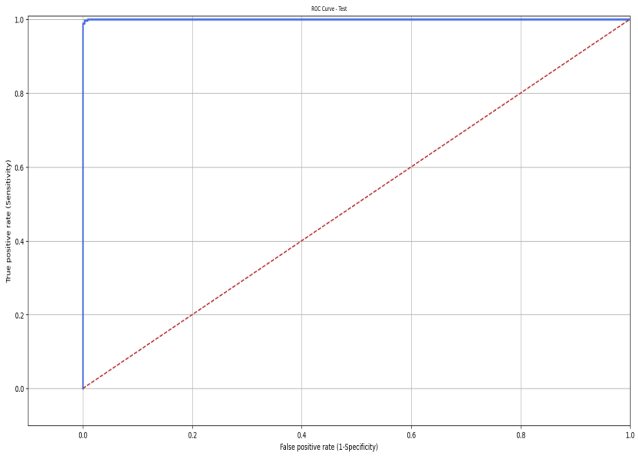

Fig. 5: The ResNet50's ROC Curve, which shows the trade-off between sensitivity and specificity for tuberculosis detection

D. Error Analysis

A thorough examination of the ResNet50 model's performance is given in Figure 6, which displays the confusion matrix for the test dataset. The classifier correctly identified 350 samples as true negatives (TB-negative) and 350 samples as true positives (correctly identified TB cases). The model produced 3 false positives, where TB-negative samples were incorrectly classified as positive. Notably, the model had 0 false negatives, where TB-positive cases are missed.

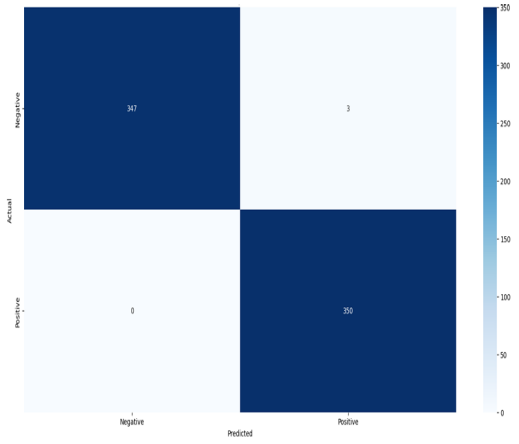

Fig. 6: Confusion Matrix Representing the Classification Performance of the ResNetB0 on Tuberculosis Detection

The classifier's capacity to discriminate between positive and negative situations was demonstrated by the error rates, which were often restricted to minimal false positives and no false negatives. These

Milestone Transactions on
MEDICAL TECHNOMETRICS
Vol. 03, Issue. 01, 2025

results demonstrate that the model is very reliable in detecting TB, exhibiting high sensitivity and specificity.

E. XAI using LIME

LIME was employed as part of the XAI framework to enhance interpretability and build trust in the ResNet50 model for TB detection. Figure 7 presents LIME-generated explanations alongside the original chest X-ray images and their segmentation masks, as shown in the visualization. The first and second rows of the figure show examples of images that were classified as 'Normal'.

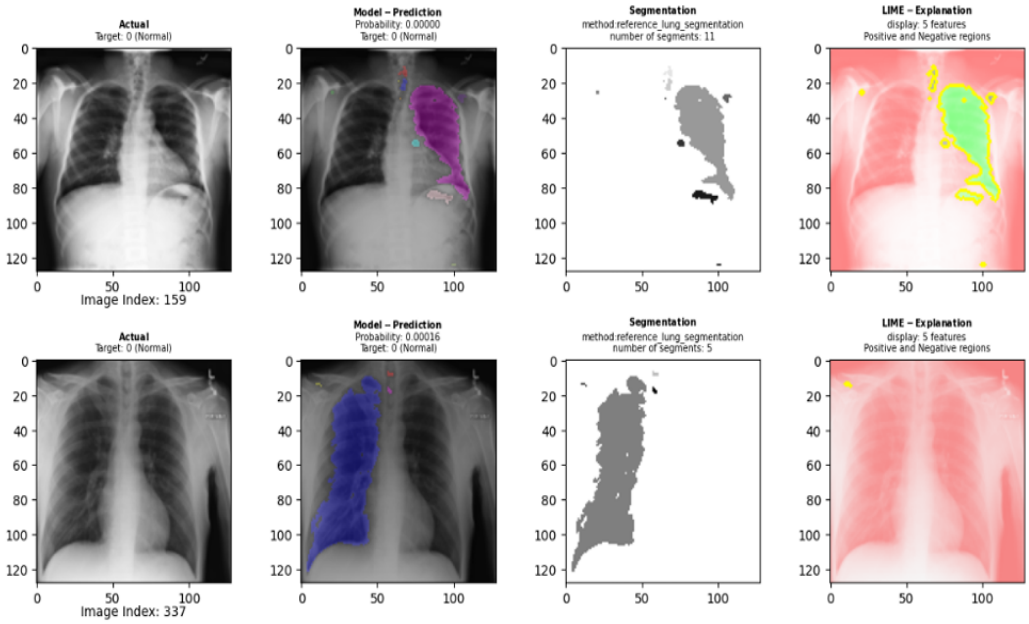

Fig. 7: LIME-based Explainability for TBNet Classifier Predictions

The following key components are shown:

- *Actual Images (Leftmost Column):* The baseline for analysis is the original chest X–rays.
- *Model Predictions (Second Column):* The classifier's confidence scores and features contributing to its prediction are highlighted in visual overlays. The areas of attention are highlighted by color-coded overlays (e.g. magenta, cyan).
- *Segmentation Maps (Third Column):* These are lung regions segmented using the reference segmentation technique, with the number of distinctive segments used in the analysis.
- *LIME Explanations (Rightmost Column):* LIME-generated heat maps show positive (green) or negative (yellow) regions that contribute to the model's predictions. Red highlighted areas are regions of high relevance to classifier decision-making.

Based on the LIME analysis, the ResNet50 model's decisions are primarily based on specific lung regions, enhancing the model's interpretability and providing a better understanding of its decision-making process. By aligning with clinical expectations, the classifier focuses on clinically relevant areas for TB

Milestone Transactions on
MEDICAL TECHNOMETRICS
Vol. 03, Issue. 01, 2025

diagnosis, thereby supporting the model's reliability for TB detection tasks. Additionally, the comparison visualizations demonstrate the strength of the ResNet50 model's predictions across various conditions, confirming the model's capacity to generalize and operate consistently over several datasets and environments. This approach provides a more transparent and reliable system for clinical usage and increases confidence in the model's forecasts.

V. CONCLUSION AND FUTURE WORK

By combining convolutional neural networks (CNNs) and improved preprocessing procedures, the ResNet50 model significantly improves diagnostic accuracy and advances tuberculosis detection by utilizing deep learning approaches. The model's predictions are made more transparent and interpretable in this study by utilizing explainable AI (XAI) approaches like LIME. The ResNet50 model builds trust with physicians and stakeholders by showing the pertinent regions of chest X-rays that guide its conclusions, thereby bridging the gap between advanced AI models and their real-world applications. Certain limitations must be acknowledged. The model's effectiveness is contingent upon access to high-quality, well-annotated datasets, rendering it susceptible to biases stemming from variations in image quality and inconsistent labeling standards. While LIME offers localized interpretability, it may not fully encompass the complexities of the decision-making process. Furthermore, challenges remain in identifying rare forms of tuberculosis, such as extrapulmonary TB. Future research should focus on enhancing dataset diversity through federated learning and international collaborations. Incorporating clinical metadata and multimodal imaging (e.g., CT scans) could improve prediction accuracy. Additionally, large-scale validation in real-world environments is essential to evaluate the model's adaptability across varied populations. Expanding the ResNet50 framework for multi-disease detection could further amplify its impact on global health.

REFERENCES

1. Rifai, A. M., Raharjo, S., Utami, E., & Ariatmanto, D. (2024). Analysis for diagnosis of pneumonia symptoms using chest X-ray based on MobileNetV2 models with image enhancement using white balance and contrast-limited adaptive histogram equalization (CLAHE). *Biomedical Signal Processing and Control, 90*, 105857.
2. Nafisah, S. I., & Muhammad, G. (2024). Tuberculosis detection in chest radiograph using convolutional neural network architecture and explainable artificial intelligence. *Neural Computing and Applications, 36*(1), 111–131.
3. Rehman, A. U., Bajwa, T. H., Bajwa, U., & Toor, W. T. (2024). Tuberculosis detection in chest X-rays using hybrid deep learning models. In *2024 3rd International Conference on Emerging Trends in Electrical, Control, and Telecommunication Engineering (ETECTE)* (pp. 1–6). IEEE.
4. Tuberculosis (TB) Chest X-ray Database. (2025, January). Retrieved January 26, 2025, from https://www.kaggle.com/datasets/tawsifurrahman/tuberculosis-tb-chest-xray-dataset.
5. Qin, Z. Z., Ahmed, S., Sarker, M. S., Paul, K., Adel, A. S. S., Naheyan, T., Barrett, R., Banu, S., & Creswell, J. (2021). Tuberculosis detection from chest X-rays for triaging in a high tuberculosis-burden setting: An evaluation of five artificial intelligence algorithms. *The Lancet Digital Health, 3*(9), e543–e554.
6. Rahman, T., Khandakar, A., Kadir, M. A., Islam, K. R., Islam, K. F., Mazhar, R., Hamid, T., Islam, M. T., Kashem, S., Mahbub, Z. B., et al. (2020). Reliable tuberculosis detection using chest X-ray with deep learning, segmentation, and visualization. *IEEE Access, 8*, 191586–191601.
7. Ahsan, M., Gomes, R., & Denton, A. (2019). Application of a convolutional neural network using transfer learning for tuberculosis detection. In *2019 IEEE International Conference on Electro Information Technology (EIT)* (pp. 427–433). IEEE.
8. Hernández, A., Panizo, A., & Camacho, D. (2019). An ensemble algorithm based on deep learning for tuberculosis classification. In *Intelligent Data Engineering and Automated Learning–IDEAL 2019: 20th International Conference, Manchester, UK, November 14–16, 2019, Proceedings, Part I* (pp. 145–154). Springer.

Milestone Transactions on
MEDICAL TECHNOMETRICS
Vol. 03, Issue. 01, 2025

9. Yadav, O., Passi, K., & Jain, C. K. (2018). Using deep learning to classify X-ray images of potential tuberculosis patients. In *2018 IEEE International Conference on Bioinformatics and Biomedicine (BIBM)* (pp. 2368–2375). IEEE.
10. Evangelista, L. G. C., & Guedes, E. B. (2018). Computer-aided tuberculosis detection from chest X-ray images with convolutional neural networks. In *Anais do XV Encontro Nacional de Inteligência Artificial e Computacional* (pp. 518–527). SBC.
11. Singh, N., & Hamde, S. (2019). Tuberculosis detection using shape and texture features of chest X-rays. In *Innovations in Electronics and Communication Engineering: Proceedings of the 7th ICIECE 2018* (pp. 43–50). Springer.
12. Prova, N. N. I. (2024). Advanced machine learning techniques for predictive analysis of health insurance. In *2024 Second International Conference on Intelligent Cyber Physical Systems and Internet of Things (ICoICI)* (pp. 1166–1170). IEEE.
13. Nguyen, Q. H., Nguyen, B. P., Dao, S. D., Unnikrishnan, B., Dhingra, R., Ravichandran, S. R., Satpathy, S., Raja, P. N., & Chua, M. C. (2019). Deep learning models for tuberculosis detection from chest X-ray images. In *2019 26th International Conference on Telecommunications (ICT)* (pp. 381–385). IEEE.
14. Hwang, E. J., Park, S., Jin, K.-N., Kim, J. I., Choi, S. Y., Lee, J. H., Goo, J. M., Aum, J., Yim, J.-J., Park, C. M., et al. (2019). Development and validation of a deep learning–based automatic detection algorithm for active pulmonary tuberculosis on chest radiographs. *Clinical Infectious Diseases, 69*(5), 739–747.
15. Sharma, V., Gupta, S. K., Shukla, K. K., et al. (2024). Deep learning models for tuberculosis detection and infected region visualization in chest X-ray images. *Intelligent Medicine, 4*(2), 104–113.
16. Chandra, T. B., Verma, K., Singh, B. K., Jain, D., & Netam, S. S. (2020). Automatic detection of tuberculosis-related abnormalities in chest X-ray images using a hierarchical feature extraction scheme. *Expert Systems with Applications, 158*, 113514.
17. Kumar, S. S., Ahmed, S. T., Xin, Q., Sandeep, S., Madheswaran, M., & Basha, S. M. (2022). Unstructured Oncological Image Cluster Identification Using Improved Unsupervised Clustering Techniques. *Computers, Materials & Continua*, *72*(1).
18. Chang, R.-I., Chiu, Y.-H., & Lin, J.-W. (2020). Two-stage classification of tuberculosis culture diagnosis using convolutional neural network with transfer learning. *The Journal of Supercomputing, 76*(11), 8641–8656.